Galactosylated Pro-Drug of Ursodeoxycholic Acid: Design, Synthesis, Characterization, and Pharmacological Effects in a Rat Model of Estrogen-Induced Cholestasis

(Article begins on next page)

01 June 2024

A GALACTOSYLATED PRO-DRUG OF URSODEOXYCHOLIC ACID: DESIGN, SYNTHESIS, CHARACTERIZATION AND PHARMACOLOGICAL EFFECTS IN A RAT MODEL OF ESTROGEN-INDUCED CHOLESTASIS

Francesca Di Guida, [1#] Claudio Pirozzi, [1#] Salvatore Magliocca, [2] Anna Santoro, [1] Adriano Lama, [1] Roberto Russo, [1] Maria Nieddu, [2] Lucia Burrai, [2] Gianpiero Boatto, [2] Maria Pina Mollica, [3] Federica Sodano, [4] Loretta Lazzarato, [4] Konstantin Chegaev, [4] Rosaria Meli, [1] Giuseppina Mattace Raso, [1*] and Maria Grazia Rimoli [1*]

[1]Department of Pharmacy, University of Naples Federico II, Naples, Italy, [2]Department of Chemistry and Pharmacy, University of Sassari, Sassari, Italy, [3]Department of Biology, University of Naples Federico II, Naples, Italy, [4]Department of Drug Science and Technology, University of Turin, Turin, Italy.

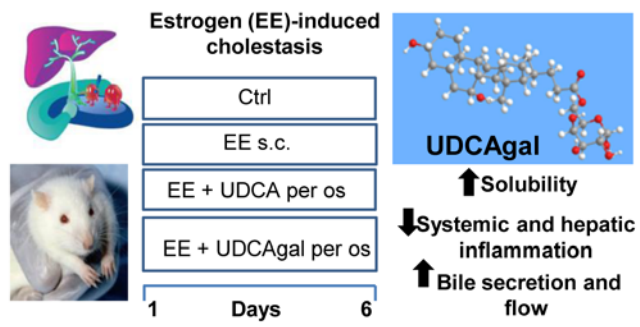[#] these authors contributed equally to this work

*These authors contributed equally to this work

Corresponding author information: Giuseppina Mattace Raso, mattace@unina.it – 081 678423;

Maria Grazia Rimoli, rimoli@unina.it - 081 678612; Department of Pharmacy, Via Domenico Montesano, 49 – 80131 Naples;

TABLE OF CONTENTS (TOC) GRAPHIC

ABSTRACT

Ursodeoxycholic acid (UDCA) is considered the first-choice therapy for cholestatic disorders. To enhance solubility and exploit specific transporters in liver, we synthesized a new galactosyl pro-drug of UDCA (UDCAgal). Ethinylestradiol (EE)-induced cholestasis was used to study and compare the effects of UDCAgal with UDCA on bile flow, hepatic canalicular efflux transporter expression, and inflammation.

UDCAgal resulted quite stable both at pH 7.4 and 1.2 and regenerated the parent drug after incubation in human plasma. Its solubility, higher than UDCA, was pH- and temperature-independent. UDCAgal displayed a higher cell permeation compared to UDCA in liver HepG2 cells. Moreover, in cholestatic rats, UDCAgal showed a higher potency compared to UDCA in reducing serum biomarkers (AST, ALT, and ALP) and cytokines (TNF-α and IL-1β). The higher effect of UDCAgal on the increase in bile salt export pump and multidrug resistance-associated protein 2 transcription indicated an improved spillover of bile acids from the liver. UDCAgal showed a reduction in CCL2, as well as TNF-α, IL-1β and cyclooxygeanse-2 mRNAs, indicating a reduction in hepatic neutrophil accumulation and inflammation. Moreover, UDCAgal, similarly to UDCA, heightens bile flow and modulates biliary acids secretion. These results indicate that UDCAgal has a potential in the treatment of cholestatic disease.

Abbreviations used: ALP, alkaline phosphatase; ALT, alanine aminotransferase; AST, aspartate aminotransferase; Bsep, bile salt export pump; CA, cholic acid; CCL2, C-C motif chemokine ligand 2; CDCA, chenodeoxycholic acid; CON, control group; DCA, deoxycholic acid; DMAP, *N,N*-dimethylpyridin-4-amine; EDC HCl, N-ethyl-N′-(3-dimethylaminopropyl) carbodiimide

hydrochloride; EE, 17α-ethinyl estradiol; HDCA, hyodeoxycholic acid; IL, interleukin; IS, internal standard (cholic acid-2,2,4,4-D4); MRM, multiple reactions monitoring; Mrp2, multidrug resistance-associated protein 2; Ntcp, sodium taurocholate cotransporting polypeptide; PBS, phosphate buffered saline; Ptgs2, cyclooxygenase-2 gene; SGF, simulated gastric fluid; UDCA, ursodeoxycholic acid; UDCAgal, ursodeoxycholic-D-galactos-6'-yl ester.

INTRODUCTION

Estrogen–induced cholestasis is one of the most common hepatopathies in many conditions of susceptible women, such as pregnancy, administration of oral contraceptives, or postmenopausal hormone replacement therapy[1-3] with limited therapeutic approach. Currently, ursodeoxycholic acid (UDCA) is used for the treatment of estrogen-induced cholestasis, such as intrahepatic cholestasis of pregnancy, but also in other transient cholestatic conditions in adult and children.[4-7] Indeed, this drug relieves pruritus, improves serum levels of aminotransferases, and decreases endogenous serum bile acid levels in women with intrahepatic cholestasis of pregnancy with a good safety profile.[8] UDCA is orally administered and is dissolved in the proximal jejunum in mixed micelles of endogenous bile acids;[9] then, is absorbed by passive non-ionic diffusion mainly in the small intestine and transported to the liver, undergoing first-pass metabolism by conjugation with aminoacids, glycine and taurine, and then secreted into bile. The clinical effectiveness of UDCA includes its choleretic activity, the capability to inhibit hydrophobic bile acid absorption by the intestine under cholestatic conditions, reducing cholangiocyte injury, stimulation of impaired biliary output, and inhibition of hepatocyte apoptosis.[10]

Despite its clinical effectiveness, UDCA is poorly soluble in the gastro-duodeno-jejunal contents and pharmacological doses of UDCA are not readily soluble in the stomach and intestine in healthy man,[11] resulting in incomplete absorption. In patients with cholestatic liver diseases, UDCA hepatic uptake and biliary secretion are impaired.[12] Numerous strategies have been proposed to overcome pharmacokinetic limits of drugs, among them, the pro-drug approach, that consists of designing pharmacologically inactive derivatives, that undergoing biotransformation, release the active drug before exhibiting their pharmacological effects. Here, we have applied this above-mentioned strategy conjugating D-galactose to the parent drug UDCA.

The galactose molecule was chosen as pro-moiety of this pro-drug in order to increase UDCA solubility in biological fluids and bioavailability, and to exploit specific transporters in liver.

Indeed, it has been demonstrated that hexoses-conjugated drugs, including galactosyl esters, once administered *per os*, are able to employ facilitate transporter systems to cross intestinal cell membrane according to their concentration gradient.[13] The transport of glycosylated compounds was demonstrated to be mostly facilitated through glucose transporters,[14] that is the dominant isoform located both on the basolateral side of enterocytes, and liver, ensuring carbohydrate absorption and liver uptake.[15] Actually, our previous studies documented the improvement of galactos-6-yl ester pro-drug permeation through cellular uptake/transport[16,17] and the amelioration of pharmacokinetic features.[18,19] Therefore, such approach was used to increase cell membrane entry of pro-drug in the enterocytes and liver cells.[20] Since glucose transporters are abundantly expressed in Kupffer and parenchymal liver cells, they could be attractive targets for the hepatic drug delivery for the treatment of liver pathologies.[21]

Consistently, we have designed, synthesized and characterized the galactosylated pro-drug of UDCA (UDCAgal) evaluating its solubility in simulated biological fluids, its chemical and plasmatic stability and its pharmacological effects in 17α-ethinylestradiol (EE)-induced cholestasis in rat compared to the parental drug. EE is a hepatotoxicant widely used in rodents to examine molecular mechanisms involved in estrogen-induced cholestasis, showing decrease in bile flow and bile acid synthesis and down-regulation in transporters and enzymes involved in bile acid homeostasis.[22] Previous data have been shown an improvement of EE-induced cholestasis by UDCA.[23,24]

EXPERIMENTAL SECTION

Drugs and Chemicals. All chemicals used for the synthesis were purchased from commercial sources (Sigma-Aldrich). The UDCA was purchased from FarmaLabor. Cholic acid (CA), chenodeoxycholic acid (CDCA), hyodeoxycholic acid (HDCA), UDCA, and IS, used as standards for liquid chromatography/tandem mass spectrometry (LC-MS-MS) analysis, were purchased from Santa Cruz Biotechnology (Dallas, Texas, U.S.A.). Deionised and distilled water was purified through a Milli-Q water system (Millipore, Billerica, MA, USA). All solvents were of the maximum level of purity and were provided by Sigma (Sigma-Aldrich, Milan, Italy). Strata C18-E (100 mg/1mL) SPE columns were purchased from Phenomenex (Torrance, CA, USA), and were mounted on a VacElut vacuum manifold (Sigma-Aldrich, Milan, Italy).

Chemistry. All reactions involving air-sensitive reagents were performed under nitrogen in oven-dried glassware using syringe-septum cap technique. Flash column chromatography was performed on silica gel (Merck Kieselgel 60, 230–400 mesh ASTM) and on RP-18 silica gel (Fluka 90, 230–400 mesh). Reactions were monitored by thin-layer chromatography (TLC) carried out on 0.25 mm Merck Kieselgel 60 F254 silica gel or Merck 60 F254 RP – 18 silica gel coated aluminium plates using subsequently two solutions: ethanol/10% vanillin and ethanol/20% sulfuric acid as visualizing agent. Unless otherwise stated, all reagents were used as received without further purifications. Dichloromethane was dried over P_2O_5 and freshly distilled under nitrogen prior to use. ^1H and ^{13}C NMR spectra were recorded on a BrukerAvance 300, at 300 and 75 MHz, respectively, using selected ion monitoring e_4 as internal standard. The following abbreviations indicate peak multiplicity: s = singlet, d = doublet, t = triplet, m = multiplet, bs = broad singlet. ESI spectra were recorded on a Micromass Quattro API micro (Waters Corporation, Milford, MA, USA) mass spectrometer. Data were processed using a MassLynxSystem (Waters). High resolution-tandem

mass spectrometry experiments were conducted on a Thermo-Fisher LTQ-Orbitrap-XL hybrid mass spectrometer system with an ION MAX API electrospray ion source in positive ion mode. Specific optical rotation, [α], were measured at 20°C in solution at a concentration of 0.5g/100mL with a Jasco P-2000 digital polarimeter at a wavelength of 589. Purity of final compound was determined by an Acquity Ultra Performance LC™, Waters Corporation Milford MA, USA, equipped with BSM, SM, CM and PDA detector. The analytical column was a Phenomenex Synergi 4U Fusion - RP, 150·2 mm· 4 µm. The mobile phase consisted of CH_3CN e NH_4OAc 1mM 50/50 v/v. UPLC retention time (t_R) was obtained at flow rates of 0.3 mL min^{-1}, and the column effluent was monitored using Micromass Quattro micro™ API Esci multi-mode ionization Enabled as detector.

Synthesis of 1,2,3,4-di-O-isopropylidene-D-α-galactopyranose-6-yl ursodeoxycholic ester. To the solution of UDCA (2.00 g, 5.09 mmol) and 1,2,3,4-di-O-isopropylidene-D-α-galactopyranose (1.32 g, 5.07 mmol), in 20 mL of pyridine / dichloromethane (1/1 v/v) mixture N-ethyl-N′-(3-dimethylaminopropyl) carbodiimide hydrochloride (EDC HCl) (1.17 g, 6.1 mmol) was added in one portion followed by N,N-dimethylpyridin-4-amine (DMAP) (32 mg, 0.26 mmol). The reaction mixture was stirred at room temperature for 24 hours. The organic phase was diluted with CH_2Cl_2 (20 mL) and washed with 2M HCl (4×25 mL), brine, dried over sodium sulphate and concentrated to dryness. The obtained yellow oil was purified by flash chromatography (eluent Hexane / EtOAc = 1 / 1 v/v), to obtain **1a** as a white solid. (Yield 2.73 g, 85%).

^{1}H NMR (300 MHz, CDCl$_3$) δ 5.53 (d, J = 5.0 Hz, 1H), 4.61 (dd, J = 7.9, 2.4 Hz, 1H), 4.34 – 4.13 (m, 4H), 4.05 – 3.98 (m, 1H), 3.57 (dd, J = 10.1, 5.5 Hz, 2H), 2.45 – 2.32 (m, 1H), 2.31 – 2.18 (m, 1H), 1.99 (d, J = 12.1 Hz, 1H), 1.93 – 1.72 (m, 5H), 1.72 – 0.99 (m, 32H), 0.94 (s, 3H), 0.92 (d, J = 6.3 Hz, 3H), 0.67 (s, 3H). ^{13}C NMR (75 MHz, CDCl$_3$) δ 174.5, 109.8, 109.0, 96.3, 71.6, 71.5, 71.2, 70.9, 70.6, 66.1, 63.4, 55.8, 55.1, 44.0, 43.9, 42.6, 40.3, 39.3, 37.5, 37.0, 35.4, 35.1, 34.2, 31.3,

31.2, 30.5, 28.7, 27.0, 26.2, 26.1, 25.1, 24.6, 23.5, 21.3, 18.5, 12.3. ESI-MS [M+Na]$^+$: m/z 657.6. [α]$_D^{20}$ = + 9.48°±0.15° (c 0.5, CH$_2$Cl$_2$).

Synthesis of D-α, β-galactopyranose-6-yl ursodeoxycholic ester. **1a** (3.44 g; 5.42 mmol) was dissolved in a solution of trifluoroacetic acid (TFA)/H$_2$O 90/10 and kept under electromagnetic stirring at room temperature for 30 minutes. The solvent was evaporated and the residue was taken up with toluene (20 mL) and concentrated under reduced pressure for two times. Obtained glassy oil was purified by flash chromatography (RP-18 silica gel eluent H$_2$O in a gradient of CH$_3$CN 70 / 30 – 60 / 40 v/v) to obtain a white foam that was taken up with methanol and precipitated with diethyl ether. Precipitate was filtered, washed with Et$_2$O and desiccated to give the flaky solid (Yield 2.63 g, 89%). ^{1}H NMR (300 MHz, CD$_3$OD) δ 5.10 and 4.40 (d, J = 3.0 Hz, 1H, C-1'), 4.24 – 4.14 (m, 2H), 3.87 – 3.67 (m, 1H), 3.52 – 3.39 (m, 3H), 2.44 – 2.29 (m, 1H), 2.29 – 2.15 (m, 1H), 2.01 (d, J = 13.3 Hz, 1H), 1.91 – 1.72 (m, 5H), 1.63 – 0.99 (m, 18H), 0.97 – 0.90 (m, 6H), 0.68 (s, 3H). ^{13}C NMR (75 MHz, CD$_3$OD) δ 175.8 and 175.7 (CO ester), 98.7 and 94.3 (C-1'), 74.8, 74.0 and 73.6 (C-3'), 72.1 and 72.0 (C-2'), 71.1 and 71.0 (C-5'), 70.4 and 70.3 (C-4'), 69.2, 66.9, 65.0 and 64.8 (C-6'), 57.5, 56.5, 44.8, 44.5, 44.0, 41.6, 40.7, 38.6, 38.0, 36.7, 36.1, 35.2, 32.2 and 31.9 (*CH$_2$CO), 31.0, 29.7, 27.9, 23.9, 22.4, 18.9, 12.6. ESI-MS [M+Na]$^+$: m/z 577.8. HRMS (ESI) calculated for C$_{30}$H$_{50}$NaO$_9$ (M+Na)$^+$ 577.3353, observed 577.3371. [α]$_D^{20}$ = +63.33°±0.16° (c 0.5, CH$_3$OH). UPLC MS purity ≥ 95% (CH$_3$CN e NH$_4$OAc 1 mM 50/50 (v/v), flow = 0.3 mL/min, t_R = 1.85 min).

Stability Tests of UDCAgal. The solutions for stability tests were prepared by dissolving an aliquot of UDCAgal in pH 7.4 phosphate buffer, in hydrochloric acid 0.1 N (pH 1) or in plasma. The solutions were maintained at 37°C and aliquots were withdrawn every hour for chromatographic analysis. To determine enzymatic stability, an aliquot of plasma was extracted

with acetonitrile (1:2) every hour and the solutions were vortexed and centrifuged at 3000 rpm (1000g) for 10 min. The supernatant (20 µL) was analyzed in LC-MS.

An Agilent (Palo Alto, CA, USA) 1100 series LC-MS instrument (LC–MSD) equipped with an autosampler (G1313A) was used for analysis. Chromatographic separation of UDCAgal, UDCA and galactose was achieved using a Phenomenex Luna C18 column (150 x 4.6 mm i.d., particle size 5 µm) fitted with a 5 µm C18 security guard cartridge (Phenomenex). For gradient elution, the two solvents were: (A) 0.1 % formic acid in H_2O and (B) 0.1 % formic acid in CH_3OH. Chromatography was undertaken using a linear gradient: from 80% B to 98% B in 5 min; change from 98% to 80% B from 5 to 12 min; a 5 min re-equilibration period at the initial conditions (20% B) and was performed before each injection. The flow rate was 0.3 mL/min. Each sample (10 µL) was injected three times. Retention times for analytes were 10.3 min for UDCA, 9.3 min for UDCAgal and 3.5 min for galactose.

MS detection was performed using an Agilent G1946 (MSD 1100) single-stage quadruple instrument equipped with an electrospray atmospheric pressure ionization source. The system was calibrated with the procedures provided by Agilent; the mass spectrometer was optimized with an infusion of the mixture of the target analytes at a flow rate of 100 µL/min. The molecular ion $[M+1]^+$ was employed for quantitative measurements of analytes. The MS conditions were: drying gas (nitrogen) heated at 350 °C at a flow rate of 9.0 mL/min; nebulizer gas (nitrogen) at 35 psi; capillary voltage in positive mode at 3000 V; fragmentor voltage at 70 V.

Aqueous Solubility. UDCA and UDCAgal solubility were determined in two pH conditions, namely at pH 1.2 with simulated gastric fluid (SGF without pepsin results in ~2.0 g/L sodium chloride and ~2.917 g/L HCl) and pH 7.4 with phosphate buffered saline (PBS) 50 mM at 25°C and 37°C. 0.2 mg of UDCA was added to buffer solutions (10 mL) and the suspensions were magnetically stirred for 2 h at 25°C or 37°C. 1 mg of UDCAgal was added to buffer solutions (1

mL) and the suspension was magnetically stirred for 2 h at 25°C or 37°C. The suspension was filtered through a 13 mm Syringe Filter w/0.45 µm polytetrafluoroethylene membrane and the filtrate was analysed by Acquity Ultra Performance LC™, Waters Corporation Milford MA, USA, equipped with BSM, SM, CM and PDA detector. The analytical column was a Phenomenex Synergi 4U Fusion - RP, 150 x 2 mm· 4 µm. The mobile phase consisted of CH_3CN e NH_4OAc 1mM 50/50 v/v. UPLC retention time (t_R) was obtained at flow rates of 0.3 mL min^{-1}, and the column effluent was monitored using Micromass Quattro micro™ API Esci multi-mode ionization Enabled as detector. The molecular ion [M-1]$^-$ was employed for quantitative measurements of analytes. The MS conditions were: drying gas (nitrogen) heated at 350 °C at a flow rate of 800 L/h; nebulizer gas (nitrogen) at 80 L/h; capillary voltage in negative mode at 3000 V; fragmentor voltage at 30 V.

Cell culture and measurement of UDCA and UDCAgal uptake. Human HepG2 cells (American Type Culture Collection, Manassas, VA, USA) were cultured in RPMI 1640 medium supplemented with 10% fetal bovine serum and 1% antibiotics (100 U/mL penicillin and streptomicin) at 37°C with 5% CO_2. The cells were grown in a humidified atmosphere containing 5% CO_2 at 37℃. Before the experiment, cells were grown in P6-dishes and cultured overnight in serum-free RPMI. The following day, the cells were treated with UDCA (100 µM), and with equimolecular concentration of UDCAgal for 30 min. The UDCA concentration was chosen on the basis of previous studies on human hepatocytes.[25] Subsequently, cell supernatant was removed and cells were lysated for the quantification of UDCA and UDCAgal uptake by LC-MS analysis. Data were normalized to protein concentration.

Ethics Statement. All procedures involving animals and their care were conducted in conformity with international and national law and policies (EU Directive 2010/63/EU for animal experiments,

ARRIVE guidelines and the Basel declaration including the 3R concept). The procedures reported here were approved by the Institutional Animal Care and Use Committee of the University of Naples Federico II and by the Ministero della Salute under protocol no. 2012/0052531. As suggested by the animal welfare protocol, all efforts were made to minimize animal suffering and to use only the number of animals necessary to produce reliable scientific data.

Animal model and treatment. Male Wistar rats weighing (330.2±3.1 g) were maintained on standard diet and water *ad libitum* and housed in a temperature controlled room under a constant 12-h light/dark cycle. Animals were randomly assigned to four experimental groups (*n* = 6 each group): 1) CON, receiving the vehicle of EE (propylene glycol) and the vehicle of drugs (PBS), for 6 days; 2) a group receiving 17-α-ethinyl estradiol (EE; 5mg/kg/*die* s.c.) for 6 days; 3) a group receiving EE and treated with UDCA (EE+UDCA, 150 mg/kg/*die per os*); 4) a group receiving EE and treated with UDCAgal (EE+UDCAgal, 212,2 mg/kg/*die per os*, the equimolecular dose of UDCA).

Surgical procedures for bile flow measurement and collection were performed on day 7 between 9 and 11 a.m. Rats were anesthetized with intraperitoneal urethane (1,2 g/kg). The bile duct was surgically exposed by a midline incision and cannulated with a polyethylene cannula inserted into the common bile duct at the sphincter of Oddi. The abdominal wall was covered with saline moist gauze, and body temperature was maintained at 37°C with a warming lamp to prevent hypothermic changes in bile flow. Therefore, bile was collected and bile flow was expressed as ml bile/120 min/g liver weight, assuming a bile density of 1 g/ml.

Analysis of bile flow and bile salt composition. After 15 min of stabilization period, biliary secretions obtained from each animal were collected in pre-weighed tubes from each rat every 30 min for 2 h. Each bile sample was diluted 10 times with Milli-Q water. A 1000 µL aliquote of the

diluted sample was then submitted to a clean-up step by using the procedure reported by Huang et al.,[26] as follows: the C18 cartridge was activated with 2 mL of methanol and 2 mL of Milli-Q water; after application of the sample, the column was washed with 2 ml of Milli-Q water and dried by passing a stream of air for 5 min. The analytes were then eluted with 4 mL of methanol, and the eluate was evaporated to dryness under a stream of nitrogen. The residue was reconstituted in 1000 µL of IS standard solution (1 µg/mL) and injected into LC-MS-MS for quantification of bile salts.

LC-MS/MS analysis of bile salts. Liquid chromatography was performed using a Perkin Elmer Flexar UHPLC pump equipped with a Perkin Elmer Flexar UHPLC autosampler (Perkin Elmer, Waltham, Massachusetts, USA). Chromatographic separation was carried out on a Sinergy C18 column (50 × 2.0 mm, 4 μm, Phenomenex, Torrance, CA, USA) fitted with a 3 μm C18 security guard cartridge (4 × 2.1 mm i.d.) (Phenomenex). A sample volume of 5 µL was injected into the LC-MS/MS system. Two solvents were used for gradient elution: (A) 0.1 % formic acid in 7.5 mM ammonium acetate buffer, adjusted to pH 7 using ammonium hydroxide, and (B) 0.1 % formic acid in CH_3OH. The gradient program was: the initial mobile phase, 30% B; 0.00-12.50 min, linear gradient from 30 to 90% B; 12.50-15.00 min, isocratic elution with 90% B; 15.01 min change from 90 to 30% B; 15.01-18.00 min, isocratic elution with 30% B (re-equilibration period at the initial conditions). The flow rate was 0.3 mL/min. Each run was replicated three times.

MS detection was performed with an Applied Biosystem MDS Sciex (Concord, Ontario, Canada) 4000 Q TRAP triple quadrupole mass spectrometer equipped with an ESI, in negative ionization mode. Data acquisition and processing were accomplished using the Applied Biosystem Analyst version 1.6 software. Qualitative analysis was performed according to retention times and MRM transitions. Quantitation was performed using the Applied Biosystem MultiQuant version 2.1 software, using the internal standard method.

The MRM transitions for the analytes and IS, their optimal MS parameters were summarized in Table 1.

Table 1. *Tandem mass spectrometric conditions*

Compound	Parent ion (*m/z*)	Fragment ions (*m/z*)	DP (V)	CE (V)	CXP (V)
CA	407.1	407.1	-130	-8	-9
CDCA	391.1	391.1	-130	-8	-9
HDCA	391.1	391.1	-130	-8	-9
UDCA	391.1	391.1	-130	-8	-9
IS	411.1	411.1	-110	-5	-11

DP: declustering potential; CXP: collision cell exit potential; CE: collision energy; CA, cholic acid; CDCA, chenodeoxycholic acid; HDCA, hyodeoxycholic acid; UDCA, ursodeoxycholic acid; IS, internal standard (cholic acid-2,2,4,4-D4).

Biochemical and serum parameters. After bile collection, the animals were euthanized, blood was collected and livers were removed and weighted and immediately stored at −80 °C for following cellular and molecular measurements. Serum alanine aminotransferase (ALT), aspartate aminotransferase (AST), and alkaline phosphatase (ALP) were analyzed by standard automated procedures, according to manufacturer's protocols (AST Flex® reagent cartridge, ALT Flex® reagent cartridge, ALP Flex® reagent cartridge, Dade Behring Inc., Newark, DE). Commercially available ELISA kits were used to determine TNF-α and IL-1β (Thermo Scientific, Rockford, IL), following the manufacturer's instructions.

RNA extraction and Real-Time PCR quantification. Total RNA, isolated from liver was extracted using TRIzol Reagent (Bio-Rad Laboratories), according to the manufacturer's instructions. cDNA was synthesized using a reverse transcription kit (Nucleospin®, MACHEREY-

NAGEL GmbH & Co, Düren, Germany) from 8 μg total RNA. PCRs were performed with a Bio-Rad CFX96 Connect Real-time PCR System instrument and software (Bio-Rad Laboratories). The PCR conditions were 15 min at 95°C followed by 40 cycles of two-step PCR denaturation at 94°C for 15 s, annealing extension at 55°C for 30 s and extension at 72°C for 30 s. Each sample contained 500 ng cDNA in 2X QuantiTech SYBRGreen PCR Master Mix and primers, *Bsep*, *Mrp2*, *Ntcp*, *Ccl2*, *Il1β*, *Tnfa*, and *Ptsg2* (Qiagen, Hilden, Germany). The relative amount of each studied mRNA was normalized to GAPDH as housekeeping gene, and the data were analyzed according to the $2^{-\Delta\Delta CT}$ method.

Statistical analysis. Data are presented as mean ± S.E.M. Statistical analysis was performed by analysis of variance test for multiple comparisons followed by Bonferroni's test to evaluate significance in differences among all groups, using Graph- Pad Prism (Graph-Pad software, San Diego, CA, USA). Statistical significance was set at $P<0.05$.

Results

General procedure for the synthesis of UDCAgal. The synthesis of UDCAgal was carried out in two steps, according to the general procedure described by Curcio et al.,[18] but slightly modified in the choice of reaction solvents in order to increase the yields. Briefly, first the esterification of UDCAwas carried out with 1,2,3,4-di-*O*-isopropylidene-D-α-galactopyranose in the presence of EDC as condensing agent and DMAP, as catalyst in dry dichloromethane (DCM) and dry pyridine (Py). Then, the ketals were completely removed in an aqueous solution of TFA;[27] the target pro-drug was obtained as a foamy white solid.(**Scheme 1**).

Scheme 1.[a] *Synthesis of UDCAgal.*
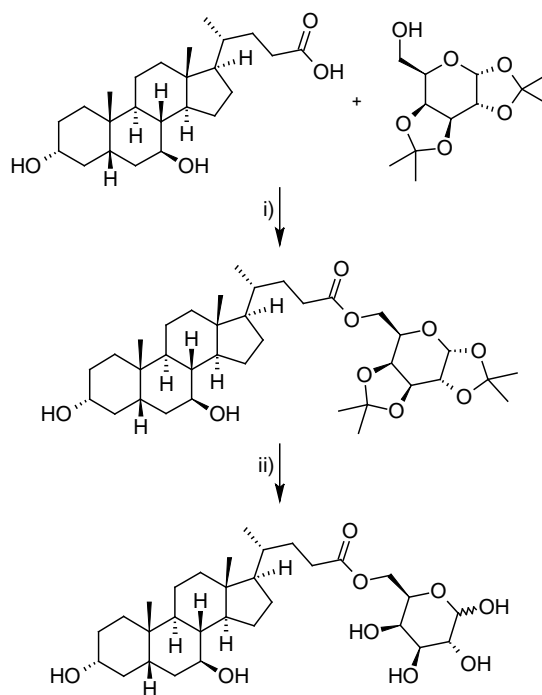
[a] Reagents and conditions: i) EDC·HCl, DMAP, DCM dry and Py dry; ii) 90% TFA in H_2O.

Stability test of UDCAgal. Regarding the chemical stability, UDCAgal appeared quite stable both at pH 7.4 (100% after 24 h) and pH 1 (74 % after 24 h). In order to determine the suitability of pro-drug to undergo enzymatic hydrolysis and hence regenerate the parent drug, UDCAgal was

incubated in human plasma. As expected, half-life time concerning enzymatic stability in plasma was lower than chemical one (Table 2).

Table 2. *Chemical and enzymatic stability of UDCAgal.*

$t_{1/2}$(**h**)		
pH=1	**pH=7.4**	**Plasma**
>24	**>24**	**0.5**

Aqueous Solubility. Aqueous solubility of UDCA and its pro-drug UDCAgal was determined at pH 7.4 in phosphate buffered saline (PBS) and pH 1.2 in SGF-without pepsin to reproduce the body fluid and the gastric environment, respectively, both at 25°C and 37°C. The solubility of UDCA in the dissolution medium was pH-dependent, in fact it increased as the pH increased, and was temperature-independent, according with Igimi and Carey. The solubility of UDCAgal was pH- and temperature-independent and was higher than UDCA; indeed, it resulted to be 0.2 mg/mL (Table 3). The ten-fold increase of UDCAgal solubility was related to the increased hydrophilicity of the galactose sugar component.

Table 3. *Solubility UDCA vs UDCAgal*

Compound	pH	Medium	Solubility, mg/mL
UDCA	1.2	SGF	< 0.02
UDCA	7.4	PBS	0.02,
UDCAgal	1.2	SGF	0.2
UDCAgal	7.4	PBS	0.2

Results are expressed as mean values (n=4).

UDCA and UDCAgal reduce serum biochemical parameters altered by EE. Preliminary experiment performed on HepG2 incubated with UDCA or the equimolar concentration of UDCAgal showed a higher uptake of UDCAgal compared to UDCA (0,318 ± 0,01 vs 0,237 ±0,01 nmol/µg protein), namely a 34% increase in UDCAgal cell entry. Serum ALT, AST, and ALP were increased by EE administration. UDCA tratment improved serum parameters (Figure 1A-C). However, UDCAgal treatment exhibited a significant higher potency than UDCA in reducing all these specific markers of liver damage altered in cholestatic rats.

All EE groups showed body weight reduction at the end of the experimental period, indicating that both treatments were not able to limit EE effect on body weight loss (data not shown). Moreover, liver weight, normalized on body weight, was increased in all EE groups, including UDCA or UDCAgal-treated ones compared to control animals (EE 3.69±0.11 and EE+UDCAgal 3.45±0.10 p<0.001, and EE+UDCA 3.57±0.21 p<0.01 vs CON 2.55±0.13).

Effects of UDCA and UDCAgal on bile flow and bile acid transport

Basal bile flow was significantly lower in rats treated with EE compared with control (Figure 2A). In particular, control and EE-treated rats had a total bile flow of 3,45±0,05 and 0,87±0,17 µL min-1, respectively, during the 120 min period of bile collection. Bile flow was partially increased after administration of UDCA or UDCAgal, as shown in Figure 2A. Then, we examined the expression of hepatic key genes which are involved in bile acid homeostasis. Firstly, we determined expression of the canalicular efflux transporters, bile salt export pump (Bsep) and multidrug resistance-related protein 2 (Mrp2), both of which are responsible for transporting hepatic bile acid into bile and constitute the limiting step of bile acid efflux. Bsep and Mrp2 expression levels were significantly reduced by EE, leading to the decrease in bile flow in rats after EE administration. UDCA, or even more UDCAgal, treatments increased Bsep and Mrp2 mRNAs (Fig. 2B and C), which resulted in

ameliorated cholestasis. Next, we determined the expression of basolateral sodium-taurocholate cotransporting peptide (Ntcp) which is involved in bile acid uptake into hepatocytes. As expected, EE markedly decreased the expression of Ntcp, as well as, both UDCA-based treatments (Fig. 2D).

Anti-inflammatory effect of UDCA and UDCAgal in serum and liver. UDCA, and, at a higher extent, UDCAgal significantly reduced serum inflammatory cytokines, TNF-α and IL-1β, up-regulated by EE administration (Figure 3 A and B). Consistently, we showed the anti-inflammatory effect of UDCA and UDCAgal treatment in liver tissue. Both compounds were able to significantly reduce mRNA expression of TNF-α, IL-1β, and cyclooxygenase-2, increased in cholestatic rats (Figure 3 C-E). Furthermore, EE insult also induced the expression of C-C motif chemokine ligand 2 (CCL2) mRNA in the liver, indicating an increase in neutrophil recruitment (Fig. 3F). Interestingly, UDCAgal effect on pro-inflammatory gene transcription in the liver was higher than UDCA.

Effects of UDCA and UDCAgal on bile salts. Bile salt excretion rate, significantly altered by EE administration, was increased by UDCA and UDCAgal, namely that of UDCA, HDCA and CDCA, except for CA, that was similar in all EE groups (Table 4).

Table 4. Effect of UDCA and UDCAgal on alterations of individual bile salt excretion rate induced by EE.

	Individual Bile Salt Output (nmol/min/g liver wt)			
	CA	**UDCA**	**HDCA**	**CDCA**
CON	$5,04\pm0,16$	$0,016\pm0,01$	$0,085\pm0,01$	$0,039\pm0,01$
EE	$0,48\pm0,13^{***}$	$0,003\pm0,01$	$0,016\pm0,01^{*}$	$0,002\pm0,01^{***}$
EE+UDCA	$0,36\pm0,01^{***}$	$0,320\pm0,01^{\#\#\#}$	$0,134\pm0,01^{\#\#}$	$0,011\pm0,01^{\#\#}$
EE+UDCAgal	$0,10\pm0,02^{***}$	$0,230\pm0,04^{\#\#\#}$	$0,098\pm0,02^{\#}$	$0,090\pm0,01^{\#\#}$

Data are expressed as mean values $\pm$ SEM (n=6 animals for each group). * $p < 0.05$ and *** $p < 0.001$ vs CON; # $p < 0.05$, ## $p < 0.01$ and ### $p < 0.001$ vs EE.

DISCUSSION

In this study, we reported data on the galactosylated pro-drug UDCAgal, accordingly with our previous papers in which we have already demonstrated the efficacy of this pharmaceutical approach *in vivo* and *in vitro* experimental models.[16,18,19,21] After the design, synthesis and characterization of galactos-6-yl ester pro-drug, we evaluated both its solubility in simulated biological fluids and chemical and enzymatic stability. The conjugation of UDCA to D-galactose causes an increment of solubility, which is related to the increased hydrophilicity of the galactose sugar component; a more soluble compound generates a drug with a better dissolution profile in biological fluids and so a grown bioavailability. UDCAgal appears quite stable both at acid and alkaline conditions; its half-life time in plasma is of about 30 minutes. Thanks to the presence of D-galactose, UDCAgal could be internalized into hepatic cells through the facilitated glucose transporters. These features of solubility and stability together with the capacity of galactosylated drugs to be internalized suggest a better pharmacokinetic profile of this UDCA releasing compound. Indeed, uptake in vitro experiments on HepG2, a human hepatocarcinoma cell line, showed an improved internalization of UDCAgal compared to UDCA, confirming other literature findings on the improved cellular uptake of galactosylated drugs. Here, we also demonstrated the efficacy of UDCAgal oral treatment in a rat model of EE-induced cholestasis. Ethinyl estradiol administration is known to increase serum markers of liver damage and to reduce bile flow, producing an impairment of transport mechanisms in both basolateral and canalicular hepatocyte membrane.[28,29] In cholestatic animals, in fact there is a reduction of bile salt excretion, bilirubin, phospholipids and cholesterol. In particular, 17α-ethinylestradiol is able to reduce both the bile salt-dependent and -independent fraction of the bile flow, in fact, mimicking estrogen-associated cholestatic disease in patients, impairs the constitutive expression of export pumps, such as Bsep [23,30,31] and Mrp2,[31,32] at the canalicular membrane of the hepatocytes, transporting bile acids into the bile.[33] The transport protein Bsep is mainly responsible for the biliary excretion of amide-conjugated bile salts, while

Mrp2 is a multispecific organic anion transporter that mediates the efflux of glucorinidated/sulfated bile acids or conjugated bilirubin, and also transports GSH.[34,35] In our experimental conditions, we observed a significant reduction in serum hepatic markers, namely ALT, AST, and ALP in cholestatic rats treated with both UDCA-based compounds, showing a better efficacy of UDCAgal. Moreover, UDCAgal was able to increase Bsep and Mrp2 transcription, even more than UDCA, indicating an increase in bile acid spillover from the liver. In fact, since bile acids and non-bile acid organic anions are the main osmotic driving force for bile flow generation, the upregulation of both transporters would contribute to the choleretic effect of UDCA and UDCAgal.

We also examined the basolateral transporter Ntcp that mediates the Na^+-dependent uptake of all physiological bile acids in their conjugated form from the portal blood supply into the hepatocytes. As already known, EE significantly decreased Ntcp mRNA expression[36] and interestingly UDCA and UDCAgal did not modify Ntcp mRNA levels that remained lower than that of controls. Indeed, it has been speculated that, after EE injection, liver cells counteract cholestasis by down-regulating their basolateral Na+-dependent bile acid uptake system, as a protective compensatory mechanism, that prevents further bile acid uptake by hepatocytes and hence hepatotoxicity. Recent studies suggest that bile acids are involved in liver injury via an inflammatory response, as neutrophil infiltration, in cholestatic rodent models,[37,38] and as cytokine increase in cultured mouse hepatocytes.[39-41] Indeed, when bile acids excretion is compromised by the alteration of bile flow from the liver, the accumulation of toxic bile acids in the liver causes cholestatic injury and progressive tissue damage.[42-45] UDCA, and, at a higher extent, UDCAgal showed a marked anti-inflammatory effect in reducing systemic and liver inflammation. Notably, CCL2 mRNA has been demonstrated to be reduced by both treatments, indicating also a reduction of neutrophil recruitment in liver tissue.

Furthermore, we have demonstrated that the treatment with the UDCAgal, as well as UDCA, was able not only to limit the alteration of bile flow, but also to increase the concentration of several bile

acids in bile. This effect highlights UDCAgal capability to restore the normal biliary bile acid secretion, favoring hepatobiliary secretion of endogenous metabolites and xenobiotics.

The evaluation of primary bile acids was performed accordingly with other studies that identify CA and CDCA as the major synthesized via the classical pathway in humans.[46] Here, we found no modification in CA levels in the bile, and a slight significant increase in CDCA amount following UDCA-based treatments. Conversely, we found a marked increase in UDCA and HDCA levels in UDCA-based treated animals. In fact, in the intestine, primary bile acids are deconjugated and modified by anaerobic microflora to secondary bile acids, mainly DCA, HDCA and lithocholic acid. The higher increase in HDCA in the rat is most likely due to the transformation of UDCA into ß-muricholic acid, and ß-muricholic acid into hyodeoxycholic during cholestasis.

Conclusion. The galactosyl pro-drug of UDCA, that is stable and more soluble than its parent drug, may represent an alternative therapy to UDCA, because it is able to preserve and enhance its systemic and hepatic anti-inflammatory activity and to improve flow and bile acids transport and composition, counteracting the progression of cholestasis and the associated liver inflammation. Moreover, the increased solubility of this pro-drug could allow the parenteral administration of UDCA in those patients with low oral compliance, affected by parenteral nutrition-associated liver disease.[47,48]

References

(1)   Williamson, C.; Miragoli, M.; Sheikh Abdul Kadir, S.; Abu-Hayyeh, S.; Papacleovoulou, G.; Geenes, V.; Gorelik, J. Bile acid signaling in fetal tissues: implications for intrahepatic cholestasis of pregnancy. *Dig Dis* **2011,** *29*, 58-61.

(2)   Paulen, M. E.; Folger, S. G.; Curtis, K. M.; Jamieson, D. J. Contraceptive use among solid organ transplant patients: a systematic review. *Contraception* **2010,** *82*, 102-12.

(3)   Vihma, V.; Ropponen, A.; Aittomaki, K.; Ylikorkala, O.; Tikkanen, M. J. Postmenopausal estrogen therapy and serum estradiol fatty acid esters in women with and without previous intrahepatic cholestasis of pregnancy. *Ann Med* **2004,** *36*, 393-9.

(4)   Lazaridis, K. N.; Gores, G. J.; Lindor, K. D. Ursodeoxycholic acid 'mechanisms of action and clinical use in hepatobiliary disorders'. *J Hepatol* **2001,** *35*, 134-46.

(5)   Kaplan, M. M.; Cheng, S.; Price, L. L.; Bonis, P. A. A randomized controlled trial of colchicine plus ursodiol versus methotrexate plus ursodiol in primary biliary cirrhosis: ten-year results. *Hepatology* **2004,** *39*, 915-23.

(6)   Paumgartner, G.; Beuers, U. Mechanisms of action and therapeutic efficacy of ursodeoxycholic acid in cholestatic liver disease. *Clin Liver Dis* **2004,** *8*, 67-81, vi.

(7)   Riely, C. A.; Bacq, Y. Intrahepatic cholestasis of pregnancy. *Clin Liver Dis* **2004,** *8*, 167-76.

(8)   Kondrackiene, J.; Beuers, U.; Kupcinskas, L. Efficacy and safety of ursodeoxycholic acid versus cholestyramine in intrahepatic cholestasis of pregnancy. *Gastroenterology* **2005,** *129*, 894-901.

(9)   Clerici, C.; Castellani, D.; Asciutti, S.; Pellicciari, R.; Setchell, K. D.; O'Connell, N. C.; Sadeghpour, B.; Camaioni, E.; Fiorucci, S.; Renga, B.; Nardi, E.; Sabatino, G.; Clementi, M.; Giuliano, V.; Baldoni, M.; Orlandi, S.; Mazzocchi, A.; Morelli, A.; Morelli, O. 3alpha-6alpha-Dihydroxy-7alpha-fluoro-5beta-cholanoate (UPF-680), physicochemical and physiological properties of a new fluorinated bile acid that prevents 17alpha-ethynyl-estradiol-induced cholestasis in rats. *Toxicol Appl Pharmacol* **2006,** *214*, 199-208.

(10)   Sanchez Pozzi, E. J.; Crocenzi, F. A.; Pellegrino, J. M.; Catania, V. A.; Luquita, M. G.; Roma, M. G.; Rodriguez Garay, E. A.; Mottino, A. D. Ursodeoxycholate reduces ethinylestradiol glucuronidation in the rat: role in prevention of estrogen-induced cholestasis. *J Pharmacol Exp Ther* **2003,** *306*, 279-86.

(11)   Parquet, M.; Metman, E. H.; Raizman, A.; Rambaud, J. C.; Berthaux, N.; Infante, R. Bioavailability, gastrointestinal transit, solubilization and faecal excretion of ursodeoxycholic acid in man. *Eur J Clin Invest* **1985,** *15*, 171-8.

(12)   Crosignani, A.; Setchell, K. D.; Invernizzi, P.; Larghi, A.; Rodrigues, C. M.; Podda, M. Clinical pharmacokinetics of therapeutic bile acids. *Clin Pharmacokinet* **1996,** *30*, 333-58.

(13)   Drozdowski, L. A.; Thomson, A. B. Intestinal sugar transport. *World J Gastroenterol* **2006,** *12*, 1657-70.

(14)   Moradi, S. V.; Varamini, P.; Toth, I. The transport and efflux of glycosylated luteinising hormone-releasing hormone analogues in caco-2 cell model: contributions of glucose transporters and efflux systems. *J Pharm Sci* **2014,** *103*, 3217-24.

(15)   Cheeseman, C. I.; Harley, B. Adaptation of glucose transport across rat enterocyte basolateral membrane in response to altered dietary carbohydrate intake. *J Physiol* **1991,** *437*, 563-75.

(16)   Melisi, D.; Secondo, A.; Montoro, P.; Piacente, S.; Rimoli, M. G.; Minale, M.; de Caprariis, P.; Annunziato, L. Galactosyl derivatives of L-arginine and D-arginine: synthesis, stability, cell permeation, and nitric oxide production in pituitary GH3 cells. *J Med Chem* **2006,** *49*, 4826-33.

(17)   Melisi, D.; Rosso, F.; Curcio, A.; Tortora, C.; Nieddu, M.; Marino, G.; Lettieri, M.; Grimaldi, A.; Luongo, E.; Romano, S.; Romano, M. F.; Boatto, G.; Abignente, E.; Barbarisi, A.;

Rimoli, M. G. Galactosyl derivative of N(omega)-nitro-L-arginine: study of antiproliferative activity on human thyroid follicular carcinoma cells. *J Cell Physiol* **2009,** *221*, 440-7.

(18)   Curcio, A.; Sasso, O.; Melisi, D.; Nieddu, M.; La Rana, G.; Russo, R.; Gavini, E.; Boatto, G.; Abignente, E.; Calignano, A.; Rimoli, M. G. Galactosyl prodrug of ketorolac: synthesis, stability, and pharmacological and pharmacokinetic evaluations. *J Med Chem* **2009,** *52*, 3794-800.

(19)   Luongo, E.; Russo, R.; Avagliano, C.; Santoro, A.; Melisi, D.; Orefice, N. S.; Raso, G. M.; Meli, R.; Magliocca, S.; Nieddu, M.; Santiago, G. M.; Boatto, G.; Calignano, A.; Rimoli, M. G. Galactosyl prodrug of palmitoylethanolamide: synthesis, stability, cell permeation and cytoprotective activity. *Eur J Pharm Sci* **2014,** *62*, 33-9.

(20)   Huttunen, K. M.; Rautio, J. Prodrugs - an efficient way to breach delivery and targeting barriers. *Curr Top Med Chem* **2011,** *11*, 2265-87.

(21)   Melisi, D.; Curcio, A.; Luongo, E.; Morelli, E.; Rimoli, M. G. D-galactose as a vector for prodrug design. *Curr Top Med Chem* **2011,** *11*, 2288-98.

(22)   Henriquez-Hernandez, L. A.; Flores-Morales, A.; Santana-Farre, R.; Axelson, M.; Nilsson, P.; Norstedt, G.; Fernandez-Perez, L. Role of pituitary hormones on 17alpha-ethinylestradiol-induced cholestasis in rat. *J Pharmacol Exp Ther* **2007,** *320*, 695-705.

(23)   Micheline, D.; Emmanuel, J.; Serge, E. Effect of Ursodeoxycholic Acid on the Expression of the Hepatocellular Bile Acid Transporters (Ntcp and bsep) in Rats With Estrogen-Induced Cholestasis. *J Pediatr Gastroenterol Nutr* **2002,** *35*, 185-91.

(24)   Li, X.; Yuan, Z.; Liu, R.; Hassan, H. M.; Yang, H.; Sun, R.; Zhang, L.; Jiang, Z. UDCA and CDCA alleviate 17alpha-ethinylestradiol-induced cholestasis through PKA-AMPK pathways in rats. *Toxicol Appl Pharmacol* **2016,** *311*, 12-25.

(25)   Komori, Y.; Arisawa, S.; Takai, M.; Yokoyama, K.; Honda, M.; Hayashi, K.; Ishigami, M.; Katano, Y.; Goto, H.; Ueyama, J.; Ishikawa, T.; Wakusawa, S. Ursodeoxycholic acid inhibits overexpression of P-glycoprotein induced by doxorubicin in HepG2 cells. *Eur J Pharmacol* **2014,** *724*, 161-7.

(26)   Huang, J.; Bathena, S. P.; Csanaky, I. L.; Alnouti, Y. Simultaneous characterization of bile acids and their sulfate metabolites in mouse liver, plasma, bile, and urine using LC-MS/MS. *J Pharm Biomed Anal* **2011,** *55*, 1111-9.

(27)   Gosenca, M.; Mravljak, J.; Gasperlin, M.; Obreza, A. The design, synthesis, and antioxidant activity of amphiphilic oximes and amidoximes. *Acta Chim Slov* **2013,** *60*, 310-22.

(28)   Gumucio, J. J.; Valdivieso, V. D. Studies on the mechanism of the ethynylestradiol impairment of bile flow and bile salt excretion in the rat. *Gastroenterology* **1971,** *61*, 339-44.

(29)   Crocenzi, F. A.; Sanchez Pozzi, E. J.; Pellegrino, J. M.; Favre, C. O.; Rodriguez Garay, E. A.; Mottino, A. D.; Coleman, R.; Roma, M. G. Beneficial effects of silymarin on estrogen-induced cholestasis in the rat: a study in vivo and in isolated hepatocyte couplets. *Hepatology* **2001,** *34*, 329-39.

(30)   Lee, J. M.; Trauner, M.; Soroka, C. J.; Stieger, B.; Meier, P. J.; Boyer, J. L. Expression of the bile salt export pump is maintained after chronic cholestasis in the rat. *Gastroenterology* **2000,** *118*, 163-72.

(31)   Trauner, M.; Arrese, M.; Soroka, C. J.; Ananthanarayanan, M.; Koeppel, T. A.; Schlosser, S. F.; Suchy, F. J.; Keppler, D.; Boyer, J. L. The rat canalicular conjugate export pump (Mrp2) is down-regulated in intrahepatic and obstructive cholestasis. *Gastroenterology* **1997,** *113*, 255-64.

(32)   Crocenzi, F. A.; D'Andrea, V.; Catania, V. A.; Luquita, M. G.; Pellegrino, J. M.; Ochoa, J. E.; Mottino, A. D.; Sanchez Pozzi, E. J. Prevention of Mrp2 activity impairment in ethinylestradiol-induced cholestasis by ursodeoxycholate in the rat. *Drug Metab Dispos* **2005,** *33*, 888-91.

(33)   Trauner, M.; Boyer, J. L. Bile salt transporters: molecular characterization, function, and regulation. *Physiol Rev* **2003,** *83*, 633-71.

(34) Dietrich, C. G.; Ottenhoff, R.; de Waart, D. R.; Oude Elferink, R. P. Role of MRP2 and GSH in intrahepatic cycling of toxins. *Toxicology* **2001,** *167*, 73-81.

(35) Kullak-Ublick, G. A.; Stieger, B.; Hagenbuch, B.; Meier, P. J. Hepatic transport of bile salts. *Semin Liver Dis* **2000,** *20*, 273-92.

(36) Gartung, C.; Schuele, S.; Schlosser, S. F.; Boyer, J. L. Expression of the rat liver Na+/taurocholate cotransporter is regulated in vivo by retention of biliary constituents but not their depletion. *Hepatology* **1997,** *25*, 284-90.

(37) Saito, J. M.; Maher, J. J. Bile duct ligation in rats induces biliary expression of cytokine-induced neutrophil chemoattractant. *Gastroenterology* **2000,** *118*, 1157-68.

(38) Gujral, J. S.; Farhood, A.; Bajt, M. L.; Jaeschke, H. Neutrophils aggravate acute liver injury during obstructive cholestasis in bile duct-ligated mice. *Hepatology* **2003,** *38*, 355-63.

(39) Allen, K.; Jaeschke, H.; Copple, B. L. Bile acids induce inflammatory genes in hepatocytes: a novel mechanism of inflammation during obstructive cholestasis. *Am J Pathol* **2011,** *178*, 175-86.

(40) Zhang, Y.; Hong, J. Y.; Rockwell, C. E.; Copple, B. L.; Jaeschke, H.; Klaassen, C. D. Effect of bile duct ligation on bile acid composition in mouse serum and liver. *Liver Int* **2012,** *32*, 58-69.

(41) Cai, S. Y.; Ouyang, X.; Chen, Y.; Soroka, C. J.; Wang, J.; Mennone, A.; Wang, Y.; Mehal, W. Z.; Jain, D.; Boyer, J. L. Bile acids initiate cholestatic liver injury by triggering a hepatocyte-specific inflammatory response. *JCI Insight* **2017,** *2*, e90780.

(42) Trauner, M.; Wagner, M.; Fickert, P.; Zollner, G. Molecular regulation of hepatobiliary transport systems: clinical implications for understanding and treating cholestasis. *J Clin Gastroenterol* **2005,** *39*, S111-24.

(43) Zollner, G.; Marschall, H. U.; Wagner, M.; Trauner, M. Role of nuclear receptors in the adaptive response to bile acids and cholestasis: pathogenetic and therapeutic considerations. *Mol Pharm* **2006,** *3*, 231-51.

(44) Wagner, M.; Zollner, G.; Trauner, M. New molecular insights into the mechanisms of cholestasis. *J Hepatol* **2009,** *51*, 565-80.

(45) Li, T.; Apte, U. Bile Acid Metabolism and Signaling in Cholestasis, Inflammation, and Cancer. *Adv Pharmacol* **2015,** *74*, 263-302.

(46) Masubuchi, N.; Sugihara, M.; Sugita, T.; Amano, K.; Nakano, M.; Matsuura, T. Oxidative stress markers, secondary bile acids and sulfated bile acids classify the clinical liver injury type: Promising diagnostic biomarkers for cholestasis. *Chem Biol Interact* **2016,** *255*, 83-91.

(47) Arslanoglu, S.; Moro, G. E.; Tauschel, H. D.; Boehm, G. Ursodeoxycholic acid treatment in preterm infants: a pilot study for the prevention of cholestasis associated with total parenteral nutrition. *J Pediatr Gastroenterol Nutr* **2008,** *46*, 228-31.

(48) Thibault, M.; McMahon, J.; Faubert, G.; Charbonneau, J.; Malo, J.; Ferreira, E.; Mohamed, I. Parenteral nutrition-associated liver disease: a retrospective study of ursodeoxycholic Acid use in neonates. *J Pediatr Pharmacol Ther* **2014,** *19*, 42-8.

Figure Captions

Figure 1. Effect of UDCA and UDCAgal on serum biochemical parameters. UDCA, and even more UDCAgal reduce total ALT (A), AST (B), and ALP (C) in EE-induced cholestasis in rat. Data are expressed as mean values ± SEM (n=6 animals for each group). *** $p < 0.001$ vs CON; ### $p < 0.001$ vs EE; § $p < 0.05$ and §§ $p < 0.01$ vs EE+UDCA.

Figure 2. UDCAgal modulates bile flow and gene expression of hepatic transporters involved in bile acid homeostasis. Evaluation of UDCA and UDCAgal effects on bile flow (A) and gene expression of *Bsep* (B), *Mrp2* (C) and *Ntcp* (D), evaluated by quantitative real-time PCR. Data are expressed as mean values ± SEM (n=6 animals for each group). *** $p < 0.001$ vs CON; # $p < 0.05$, ## $p < 0.01$ and ### $p < 0.001$ vs EE; § $p < 0.05$ vs EE+UDCA.

Figure 3. Anti-inflammatory activity of UDCAgal in serum and liver tissue. UDCAgal significantly decreases serum levels of TNF-α (A) and IL-1β (B) and mRNA expression of *Tnfa* (C), *IL1β* (D), *Ptgs2* (E), and *Ccl2* (F) in liver, all induced by EE administration. Data are expressed as mean values ± SEM (n=6 animals for each group). *** $p < 0.001$ vs CON; # $p < 0.05$, ## p < 0.01 and ### $p < 0.001$ vs EE; § $p < 0.05$ and §§§ $p < 0.001$ vs EE+UDCA (150 mg/kg).
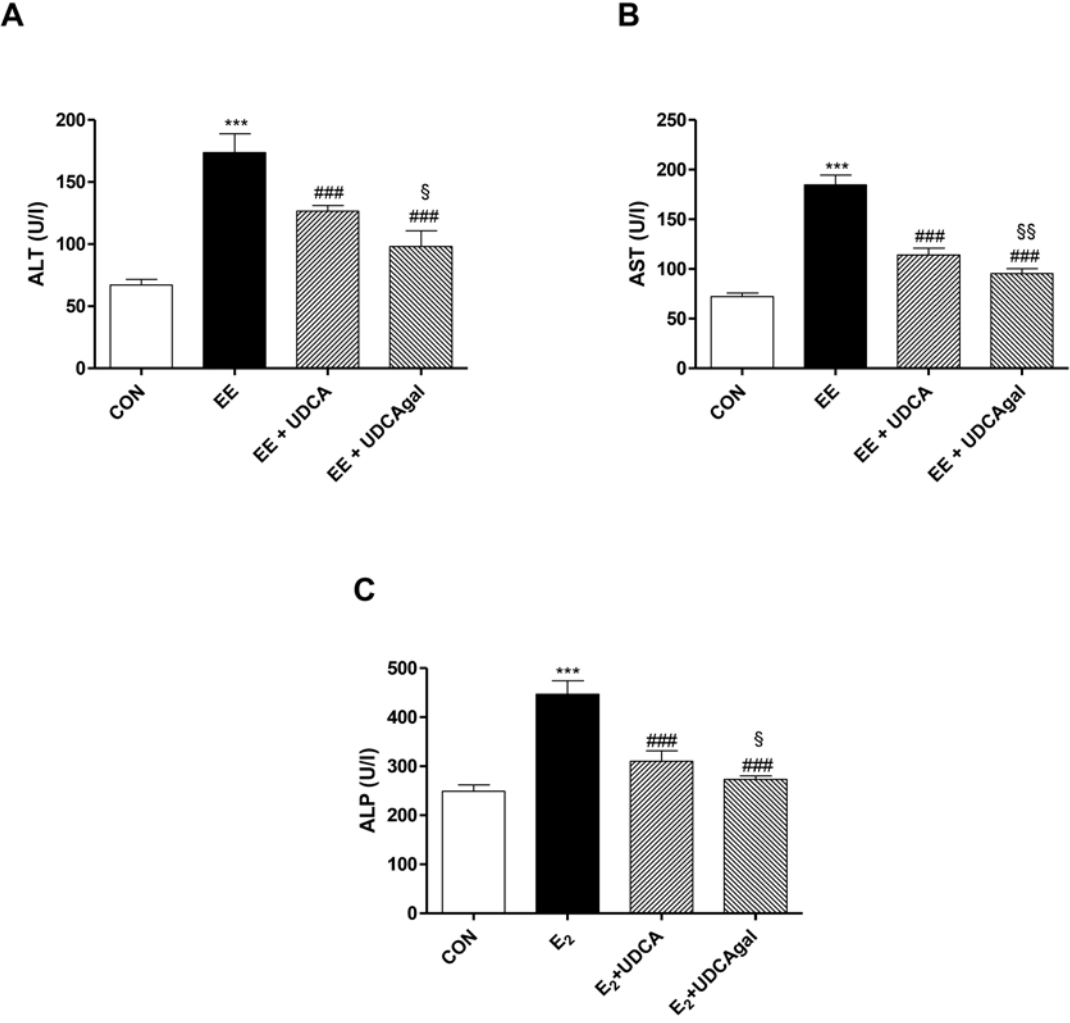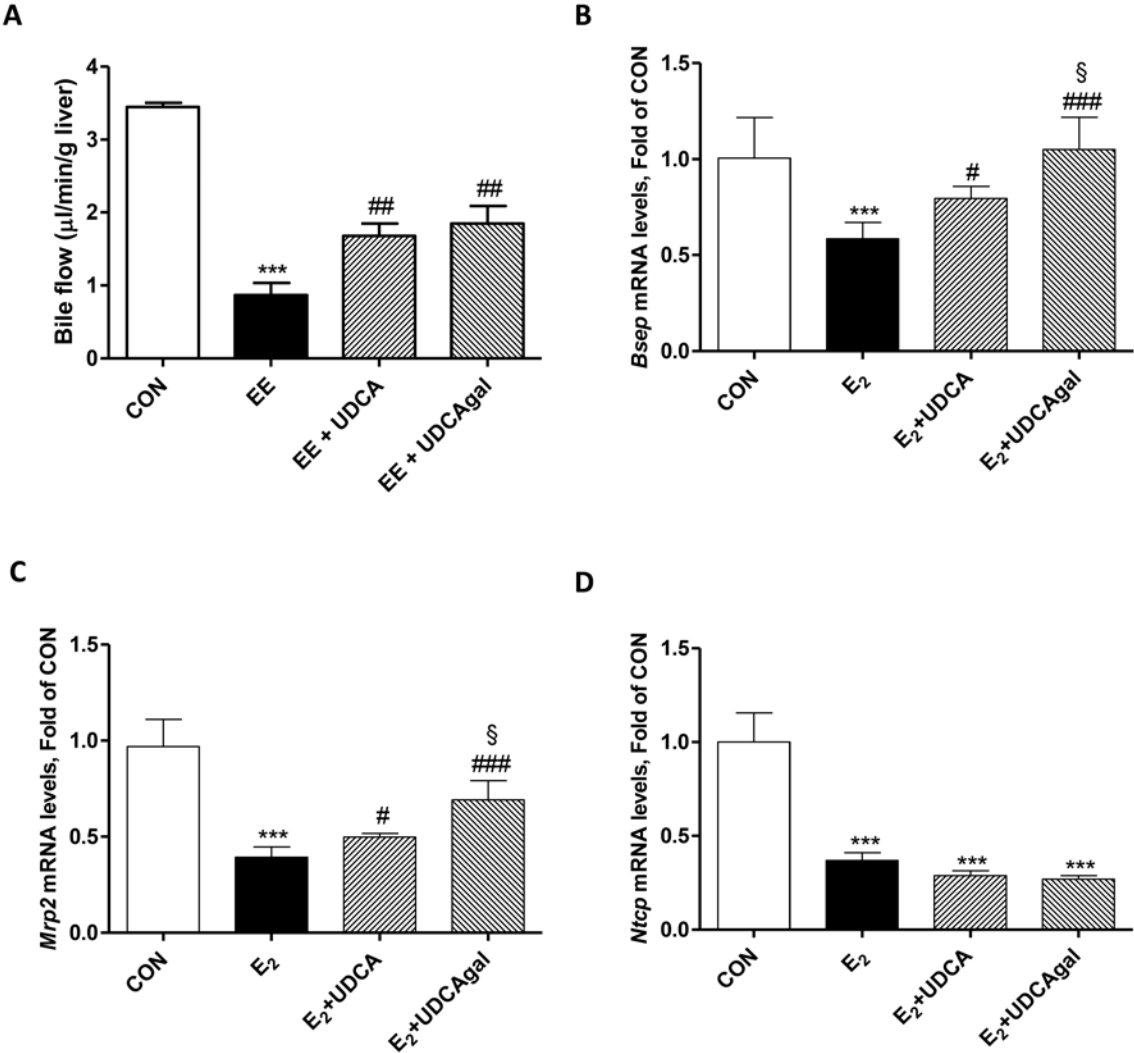
Figure 1.

Figure 2.

Figure 3.